Partial Difference Equations over Graphs: Morphological Processing of Arbitrary Discrete Data

Vinh-Thong Ta*, Abderrahim Elmoataz, and Olivier Lézoray

University of Caen Basse-Normandie, GREYC CNRS UMR 6072, Image Team
6 Boulevard Maréchal Juin, F-14050 Caen Cedex France
{vinhthong.ta,abderrahim.elmoataz-billah,olivier.lezoray}@unicaen.fr

Abstract. Mathematical Morphology (MM) offers a wide range of operators to address various image processing problems. These processing can be defined in terms of algebraic set or as partial differential equations (PDEs). In this paper, a novel approach is formalized as a framework of partial difference equations (PdEs) on weighted graphs. We introduce and analyze morphological operators in local and nonlocal configurations. Our framework recovers classical local algebraic and PDEs-based morphological methods in image processing context; generalizes them for nonlocal configurations and extends them to the treatment of any arbitrary discrete data that can be represented by a graph. It leads to considering a new field of application of MM processing: the case of high-dimensional multivariate unorganized data.

1 Introduction

Mathematical Morphology (MM) offers an important variety of tools in image processing and computer vision. The two fundamental operators are *dilation* and *erosion*.

In standard flat (algebraic) MM, these operations employ a so-called *structuring element* B to process images. Dilation (δ) and erosion (ε) of an image, represented as a scalar function $f^0 : \Omega \subset \mathbb{R}^2 \rightarrow \mathbb{R}$, by a symmetric structuring element B are defined as $\delta\left(f^0(x_i, y_i)\right) = \max\{f^0(x_i + x_j, y_i + y_j) : (x_j, y_j) \in B\}$ and $\varepsilon\left(f^0(x_i, y_i)\right) = \min\{f^0(x_i + x_j, y_i + y_j) : (x_j, y_j) \in B\}$, with $(x_i, y_i) \in \Omega$. The combination of these two operators gives rise to a variety of other MM operators; for instance opening, closing, top hats, reconstruction [1].

An alternative formulation, based on partial differential equations (PDEs), was also proposed by [2–4] and references therein. PDEs-based approach generate flat dilation and erosion of a function f, by a unit ball $B = \{z \in \mathbb{R}^2 :$

* This work was partially supported under a research grant of the ANR Foundation (ANR-06-MDCA-008-01/FOGRIMMI) and a doctoral grant of the Conseil Régional de Basse-Normandie and of the Cœur et Cancer association in collaboration with the Department of Anatomical and Cytological Pathology from Cotentin Hospital Center.

$\|z\|_p \leq 1\}$, with the following diffusion equations: $\delta_t(f) = \partial_t f = +\|\nabla f\|_p$ and $\varepsilon_t(f) = \partial_t f = -\|\nabla f\|_p$ where $\nabla = (\partial x, \partial y)^T$ is the spatial gradient operator, f is the transformed version of the image f^0 and the initial condition is $f(x, y, 0) = f^0(x, y, 0)$ at time $t = 0$. These PDEs produce continuous scale morphology and have several advantages. They offer excellent results for non-digitally scalable structuring elements whose shapes cannot be correctly represented on a discrete grid and they also allow sub-pixel accuracy. They can be adaptive by introducing a local speed evolution term [5]. However, these methods have several drawbacks. The numerical discretization is difficult for high-dimensional data or irregular domains. They only consider local interactions on the data by using local derivatives while nonlocal schemes have recently received a lot of attention [6–9]. Indeed, these latter works have shown their effectiveness in many computer vision tasks. Moreover, MM is a well known and well documented approach for binary and grayscale images. Nevertheless, there no exist general extension for the treatment of multivariate and high-dimensional data sets. Several methods address this problem such as [10] but for the particular case of tensor images or [11] for data set and cluster analysis. The latter approach uses only binary MM and has the drawback that it requires the construction of a regular discrete grid to perform MM processing. Inspired by previous work in [9], we propose to consider MM processing over graphs. Graph morphology was already defined in [12, 13] but, only algebraic MM operations and particular graphs (binary graph, minimum spanning tree) are considered. Our work is different.

Contributions. We extend the PDEs-based MM operators to a discrete scheme by considering partial difference equations (PdEs) over weighted graphs of the arbitrary topologies. To this aim, nonlocal discrete derivatives on graphs are introduced to transcribe MM processing based on the continuous PDEs to PdEs over graphs. Our approach of MM operations has several advantages. Any discrete domain that can be described by a graph can be considered without any spatial discretization. Local and nonlocal processing are naturally and directly enabled within a same formulation. These two points provides novel application fields of MM operations such as unorganized high-dimensional data processing and nonlocal MM processing for images.

Paper organization. Section 2 recalls some definitions and notations on graphs. Section 3 introduces the family of weighted nonlocal dilation and erosion. The potential of this framework is illustrated in Sect. 4, for the processing of unorganized data and in the context for image processing, on Region Adjacency Graph and textured images.

2 Mathematical Preliminaries on Graphs

2.1 Definitions and Notations

We consider any general discrete domain as a weighted graph. Let $G = (V, E, w)$ be a *weighted graph* composed of a finite set V of *vertices*, and a finite set $E \subset V \times V$ of weighted *edges*, and a *weight function* $w : V \times V \to \mathbb{R}^+$. An *edge*

of E, which connects two adjacent vertices u and v, is noted uv. In this paper, graphs are assumed to be connected and undirected (see in [14] for more details). This implies that the weight function w is symmetric, w_{uv}=w_{vu}, if $uv \in E$ and w_{uv}=0 otherwise. Let $\mathcal{H}(V)$ be the Hilbert space of real-valued functions on the vertices. This space is endowed with the usual inner product. Each function $f : V \to \mathbb{R} \in \mathcal{H}(V)$, assigns a real value $f(u)$ to each vertex $u \in V$.

Graph construction. Any discrete domain can be modeled by a weighted graph and by defining an initial function $f^0 : V \to \mathbb{R}$ on the vertices. In image processing, graphs are commonly used to represent digital images. In machine learning community, they are usually used to represent data sets and their relations. Many typical structures can be quoted. (i) *k-adjacency grid graphs* [15]: vertices represent pixels and edges represent local pixel adjacency relationship. Two common graphs are the 4 and the 8-adjacency grid graph. (ii) *Region Adjacency Graphs (RAG)* [16] that provide useful descriptions of the picture structure: vertices represent image regions and edges represent region adjacency relationship. (iii) *Proximity graphs* [17], for instance the k-Nearest Neighbors graph (k-NN graph), where each vertex is associated with a set of k close vertices depending on a similarity criterion. Constructing a graph consists in modeling the neighborhood or the similarity relationship between data. This similarity depends on a pairwise distance measure. Computing distances between data elements consists in comparing their features that generally depend on the initial function f^0. To this aim, each vertex $u \in V$ is assigned with a feature vector denoted by $F(f^0, u) \in \mathbb{R}^n$ (several choices can be considered for the expression of F and the simplest one is $F(f^0, u) = f^0(u)$). For an edge $uv \in E$, the following standard weight function $g : V \times V \to \mathbb{R}^+$ can be used

$$g_1(uv) = \big(\rho\left(F(f^0, u), F(f^0, v)\right) + \epsilon\big)^{-1}, \epsilon > 0, \epsilon \to 0 \text{ and}$$
$$g_2(uv) = \exp\left(-\rho\left(F(f^0, u), F(f^0, v)\right)^2 / \sigma^2\right) \ ,$$

where σ controls the similarity and $\rho : V \times V \to \mathbb{R}^+$ is a distance measure. Then, the choice of the graph topology enables several processing that model local or nonlocal interactions between data (especially for the image processing context). Both notions of local and nonlocal interactions are directly integrated into edges weights by the associated weight function w. One has to note that both local and nonlocal interactions are only expressed by the graph topology in terms of neighborhood connectivity (see [9] for more details on these notions).

2.2 Discrete Derivatives and Gradient Operators

We introduce discrete operators definitions such as derivatives, gradient operators and its norms. These formulations constitute the basis of our morphological operators framework.

We consider the *directional derivative* of a function $f : V \to \mathbb{R} \in \mathcal{H}(V)$ at vertex u along an edge uv. Following the basic operator defined in [9], we have

$$\left.\frac{\partial f}{\partial (uv)}\right|_u = \partial_v f(u) = w_{uv}^{1/2}\big(f(v) - f(u)\big) \ . \tag{1}$$

This definition is consistent with the continuous definition of the derivative of a function and satisfies the following properties: $\partial_v f(u) = -\partial_u f(v)$, $\partial_u f(u) = 0$, and if $f(u) = f(v)$ then $\partial_v f(u) = 0$. From (1), we introduce two other directional derivatives based on min and max operators:

$$\partial_v^+ f(u) = \max\big(0, \partial_v f(u)\big) \text{ and } \partial_v^- f(u) = \min\big(0, \partial_v f(u)\big) \ .$$

The *weighted gradient operator* of a function $f \in \mathcal{H}(V)$ at vertex $u \in V$ is the vector of all partial derivatives with respect to the set of edges uv: $(\nabla_w f)(u) = (\partial_v f(u))_{uv \in E}$. Then, with this definition one obtains:

$$(\nabla_w^+ f)(u) = \big(\partial_v^+ f(u)\big)_{uv \in E} \text{ and } (\nabla_w^- f)(u) = \big(\partial_v^- f(u)\big)_{uv \in E} \tag{2}$$

In the sequel, we use the $\mathcal{L}^p$-norm of the two latter gradients defined in (2)

$$\begin{aligned} \|(\nabla_w^+ f)(u)\|_p &= \Big[\sum_{v \sim u} w_{uv}^{p/2} \big|\max\big(0, f(v) - f(u)\big)\big|^p\Big]^{1/p} \text{ and} \\ \|(\nabla_w^- f)(u)\|_p &= \Big[\sum_{v \sim u} w_{uv}^{p/2} \big|\min\big(0, f(v) - f(u)\big)\big|^p\Big]^{1/p} \ ; \end{aligned} \tag{3}$$

and the $\mathcal{L}^\infty$-norm

$$\begin{aligned} \|(\nabla_w^+ f)(u)\|_\infty &= \max_{v \sim u}\Big(\sqrt{w_{uv}}\big|\max\big(0, f(v) - f(u)\big)\big|\Big) \text{ and} \\ \|(\nabla_w^- f)(u)\|_\infty &= \max_{v \sim u}\Big(\sqrt{w_{uv}}\big|\min\big(0, f(v) - f(u)\big)\big|\Big) \ . \end{aligned} \tag{4}$$

Similar definitions can be provided for the norm of the gradient $\nabla_w f$

3 PdEs for Morphology on Weighted Graphs: Dilation and Erosion Processes

In this Section, we define the discrete analogue of the continuous PDEs-based dilation and erosion formulations of a given function $f \in \mathcal{H}(V)$. To this aim, we use on the one hand, the decomposition of f into its level sets $f^k = H(f - k)$ where H is the Heaviside function (a step function) and on the other hand, the notion of graph boundary. Let $G = (V, E, w)$ be a graph and let A be a set of connected vertices with $A \subset V$ i.e. for all $u \in A$, there exists $v \in A$ such that $uv \in E$. We denote by $\partial^+ A$ and $\partial^- A$ respectively the *outer* and the *inner* boundary sets of A in G. Then, for a given vertex $u \in V$:

$$\partial^+ A = \big\{u \in A^c : \exists v \in A, v \sim u\big\} \text{ and } \partial^- A = \big\{u \in A : \exists v \in A^c, v \sim u\big\} \ , \tag{5}$$

where $A^c = V \setminus A$ is the complement of A. Figure 1 illustrates these notions on a 4-adjacency image grid graph and on an arbitrary graph. One can note that the boundary of V cannot be directly defined by (5). In this case, one assumed that is given. Then, dilation over A can be interpreted as a growth process that

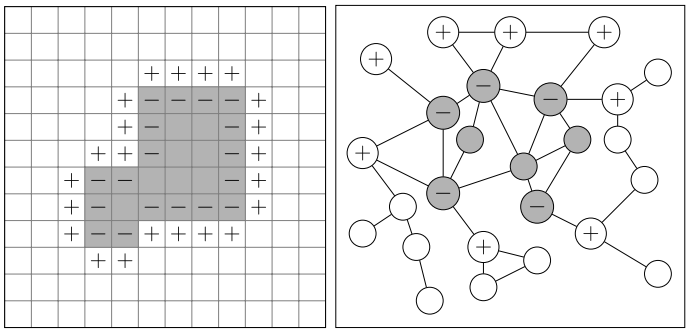

(a) 4-adjacency image grid graph (b) Arbitrary undirected graph

Fig. 1. Graph boundary on two different graphs. *Gray vertices* correspond to set A. *Plus* or *minus* vertices are respectively outer $\partial^+ A$ and inner $\partial^- A$ sets.

adds vertices from $\partial^+ A$ to A. By duality, erosion over A can be interpreted as a contraction process that removes vertices from $\partial^- A$. The following proposition shows the relation between the graph boundary and the gradients of the level set function $\|(\nabla_w^+ f^k)(u)\|_p$ and $\|(\nabla_w^- f^k)(u)\|_p$.

Proposition 1. *For any level set f^k, gradient norms* (3) *are defined by*

$$\begin{aligned} \|(\nabla_w^+ f^k)(u)\|_p &= \Big[\sum_{v\sim u, v\in A^k} w_{uv}^{p/2} \Big]^{1/p} \chi_{\partial^+ A^k}(u) \text{ and} \\ \|(\nabla_w^- f^k)(u)\|_p &= \Big[\sum_{v\sim u, v\in A^k} w_{uv}^{p/2} \Big]^{1/p} \chi_{\partial^- A^k}(u) \ , \end{aligned} \tag{6}$$

where $A^k \subset V$ is the set with $f^k = \chi_{A^k}$ and $\chi : V \to \{0,1\}$ is the indicator function.

Proof. We prove the first relation in (6). If $f^k = \chi_{A^k}$, then

$$\|(\nabla_w^+ f^k)(u)\|_p \overset{(3)}{=} \Big[\sum_{v\sim u} w_{uv}^{p/2} \big|\max\big(0, \chi_{A^k}(v) - \chi_{A^k}(u)\big)\big|^p \Big]^{1/p} \ .$$

We study the cases where $u \in A^k$, $u \notin A^k$ and similarly with the neighborhood of u. The only case where the quantity $\chi_{A^k}(v) - \chi_{A^k}(u) > 0$ is, when for a $u \notin A^k$ and its neighbor $v \in A^k$. This configuration corresponds to the definition of the outer set of vertices $\partial^+ A^k$ defined in (5). Then, with this property one can deduce the following relation:

$$\|(\nabla_w^+ f^k)(u)\|_p = \Big[\sum_{v\sim u, v\in A^k} w_{uv}^{p/2} \Big]^{1/p} \chi_{\partial^+ A^k}(u) \ .$$

Second relation in (6) is deduced by the same scheme: the only case where $\chi_{A^k}(v) - \chi_{A^k}(u) < 0$ is when we consider the inner set of vertices $\partial^- A^k$ (i.e. $u \in A^k$ and $v \notin A^k$). □

From Proposition (1) we can directly obtain the following one.

Proposition 2. *For any level set f^k and at vertex $u \in V$, the $\mathcal{L}^p$-norm of the gradient $(\nabla_w f^k)(u)$ can be decomposed as $\|(\nabla_w f^k)(u)\|_p = \|(\nabla^+ f^k)(u)\|_p + \|(\nabla^- f^k)(u)\|_p$.*

Proof. Using the inner $\partial^+ A^k$ and the outer $\partial^- A^k$ set of vertices and Proposition (1), we have:

$$\begin{aligned}\|(\nabla_w f^k)(u)\|_p &= \Big[\sum_{\substack{v\sim u\\ u\in\partial^+ A^k}} w_{uv}^{\frac{p}{2}} \big|f^k(v)-f^k(u)\big|^p\Big]^{\frac{1}{p}} + \Big[\sum_{\substack{v\sim u\\ u\in\partial^- A^k}} w_{uv}^{\frac{p}{2}} \big|f^k(v)-f^k(u)\big|^p\Big]^{\frac{1}{p}} \\ &= \|(\nabla_w^+ f^k)(u)\|_p + \|(\nabla_w^- f^k)(u)\|_p \ .\end{aligned}$$

□

Remark 1. Propositions (1) and (2), only consider the $\mathcal{L}^p$-norms. For the $\mathcal{L}^\infty$-norm one can demonstrate and obtain the same results by using expressions defined in (4).

As for the continuous case, a simple variational definition of dilation applied to f^k can be interpreted as maximizing a surface gain proportional to $+\|(\nabla_w f^k)(u)\|_p$. Similarly, erosion can be viewed as minimizing a surface gain proportional to $-\|(\nabla_w f^k)(u)\|_p$. From Proposition (2), if we consider the case where $u \in \partial^+ A^k$, $\|(\nabla_w f^k)(u)\|_p$ is reduced to $\|(\nabla_w^+ f^k)(u)\|_p$ and corresponds to dilation over A^k. This process can be expressed by the following evolution equation $\partial_t f^k(u) = +\|(\nabla_w^+ f^k)(u)\|_p$. With same scheme, the erosion process is expressed by the equation $\partial_t f^k(u) = -\|(\nabla_w^- f^k)(u)\|_p$. Finally, by extending these two processes for all the levels of f, we can naturally consider the following two families of dilation and erosion. These two processes are parameterized by p and w, over any weighted graph $G = (V, E, w)$. They are defined as

$$\begin{aligned}\delta_{p,t}(f(u)) &= \partial_t f(u,t) = +\|(\nabla_w^+ f)(u,t)\big\|_p \text{ and} \\ \varepsilon_{p,t}(f(u)) &= \partial_t f(u,t) = -\|(\nabla_w^+ f)(u,t)\big\|_p \ .\end{aligned} \tag{7}$$

Dilation process algorithm. To solve the PdEs dilation and erosion processes (7), on the contrary to the PDEs case, no spatial discretization is needed thanks to derivatives directly expressed in a discrete form. Then, one obtains the general iterative scheme for dilation, at time $t+1$, for all $u \in V$

$$f(u,t+1) = f(u,t) + \Delta t \|(\nabla_w^+ f)(u,t)\|_p \tag{8}$$

where $f(.,t)$ is the parametrization of f by an artificial time $t > 0$. The initial condition is $f(u,0) = f^0(u)$ where $f^0 \in \mathcal{H}(V)$ is the initial function defined on the graph vertices. With the corresponding gradient $\nabla_w^+ f$ norms, (8) becomes for $\mathcal{L}^p$ and $\mathcal{L}^\infty$-norms

$$f(u,t+1) \overset{(3)}{=} f(u,t) + \Delta t \Big(\sum_{v\sim u} w_{uv}^{p/2} \big|\max\big(0, f(v,t) - f(u,t)\big)\big|^p\Big)^{1/p} \text{ and} \tag{9}$$

$$f(u,t+1) \overset{(4)}{=} f(u,t) + \Delta t \max_{v\sim u}\Big(w_{uv}^{1/2} \big|\max\big(0, f(v,t) - f^n(u,t)\big)\big|\Big) \ . \tag{10}$$

The extension to erosion process case can be established by following the corresponding gradient $\nabla_w^- f$ norms in (3) and (4).

The proposed dilation and erosion framework has several advantages. (i) No spatial discretization is needed in contrary to the continuous case. (ii) The choice of a weight function provides a natural adaptive scheme by including more information on edges and repetitive structures in the processing. Local and nonlocal configurations are unified within same formulation. (iii) The same scheme works on graph of arbitrary structure i.e. any discrete data that can be represented by a graph can be processed with our framework.

Relations with image processing schemes. We show that with an adapted graph topology and an appropriated weight function, the propose methodology for dilation and erosion is linked to well-known methods defined in the context of image processing. For simplicity we only consider dilation, but same remarks apply for erosion.

Remark 2. When p=2 and the weight function is constant (i.e. w=1), one recovers from (9) the exact Osher and Sethian first-order upwind discretization scheme [18] for a grayscale image defined as $f : V \subset \mathbb{R}^2 \to \mathbb{R}$. Let $G = (V, E, 1)$ be a 4-adjacency grid graph associated to the grayscale image. From (9), we have:

$$f(u, t{+}1) \overset{w=1,p=2}{=} f(u,t) + \Delta t \Big[\sum_{v \sim u} |\max\big(0, f(v,t) - f(u,t)\big)|^2 \Big]^{1/2} .$$

Replacing the vertex u and its neighborhood by their spatial image coordinates (x, y) and following the property $\big(\max(0, a{-}b)\big)^2 = \big(\min(0, b{-}a)\big)^2$, we have

$$\begin{aligned} f((x,y),t{+}1) = f((x,y),t) + \Delta t \Big[& |\min\big(0, f((x,y),t) - f((x{-}1,y),t)\big)|^2 + \\ & |\max\big(0, f((x{+}1,y),t) - f((x,y),t)\big)|^2 + \\ & |\min\big(0, f((x,y),t) - f((x,y{-}1),t)\big)|^2 + \\ & |\max\big(0, f((x,y{+}1),t) - f((x,y),t)\big)|^2 \Big]^{\frac{1}{2}} . \end{aligned}$$

One can also note that this discretization corresponds exactly to the Osher and Sethian discretization scheme used by the PDEs-based dilation process. Using this expression, the proposed morphological framework can perform sub-pixel approximation. The notion of structuring elements as defined by [2] is recovered. For a unit ball $B = \big\{ z \in \mathbb{R}^2 : \|z\|_p \leq 1 \big\}$, if we consider the three special cases of $p = 1, 2, \infty$, an approximation of a square, circle and diamond is obtained.

Remark 3. We study the case where p=∞, with a constant weight function (i.e. w=1) and a constant time discretization (i.e. Δt=1). Our formulation recovers the classical algebraic flat morphological dilation formulation over graphs. From (10) we have

$$f(u, t{+}1) = f(u,t) + \max_{v \sim u} \Big(\max\big(0, f(v,t) - f(u,t)\big) \Big) .$$

If $f(v,t)-f(u,t) \leq 0$ then $f(u,t+1)=f(u,t)$. If $f(v,t)-f(u,t) > 0$ then we obtain $f(u,t+1) = f(u,t)+\max\limits_{v\sim u}\big(f(v,t)-f(u,t)\big) = f(u,t)+\max\limits_{v\sim u}\big(f(v,t)\big)-f(u,t)$. For both cases, by considering the neighborhood of vertex u includes u itself, then we recover the classical algebraic dilation over graphs

$$f(u,t+1) = \max_{v\sim u}\big(f(v,t)\big) \ .$$

In this case, the structuring element is provided by the graph topology and the vertices neighborhoods. For instance, if we consider an 8-adjacency image grid graph, it is equivalent to a dilation by a square structuring element of size 3×3.

4 Experimental Results

The proposed morphological framework can be used to process any function defined on the vertices of a graph or on any arbitrary discrete domain. In this Section, we illustrate our methodology through basic operations such as dilation, erosion, opening and closing. For a function $f \in \mathcal{H}(V)$, the simplest way to obtain opening and closing operations is to implement them serially as compositions of dilation δ and erosion ϵ. Then, opening is $\delta\big(\epsilon(f)\big)$ and closing is $\epsilon\big(\delta(f)\big)$.

In the sequel, to show the flexibility and the novelty of our framework, we provide examples of morphological operations on arbitrary discrete data. We also consider various graph topologies, and local and nonlocal interactions.

- Morphological image processing results are presented and in particular fast image processing. Indeed, the proposed formulation allows to consider another image representation than usual grid graph such as RAG. That leads to decrease computation complexity while obtains similar processing behavior.
- Processing results on textured images illustrate the benefits on fine and repetitive structures preservation of nonlocal interactions as compared to local one.
- Morphological processing results on high-dimensional unorganized discrete data show the potential of our framework to perform processing on arbitrary discrete domain.

For all the examples we restrict ourselves to the case of p=2 for simplicity. The objective of the following experiments is not to solve a particular application or problem. They only illustrate the potential and the behavior of our morphological framework.

Remark 4. In the case of vector-valued a function $f: V \rightarrow \mathbb{R}^n$, with $f=(f_i)_{i=1,\ldots,n}$, morphological operations are performed on each component f_i independently. This comes to have n morphological processes where the inner correlation between the vectorial data is expressed by the weight function that acts as a coupling term.

Image processing on grid graph and fast processing on RAG. This experiment compares the behavior of our proposed morphological operations for

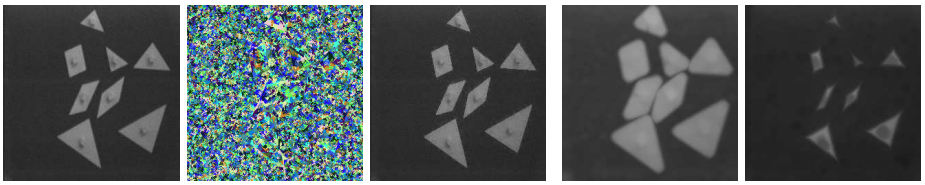

(a) Original (b) Partition (c) Reconstructed image (d) Unweighted processing on grid graph

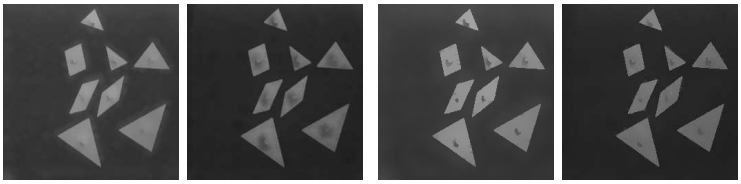

(e) Weighted processing on grid graph (f) Weighted processing on RAG

Fig. 2. Dilation and erosion on image-based graph. (a) original image (65 536 pixels). (b) partition (11 853 regions i.e. 82% of reduction). (c) reconstructed image. (d), (e) and (f) at left dilation and at right erosion. (d) and (e) unweighted and weighted operations performed on grid graph constructed from (a). (f) weighted operations performed on a RAG constructed from (b) and (c).

image processing by considering different weight functions and graph structures. Figure 2(a) presents an original scalar grayscale image considered as a function $f^0 : V \subset \mathbb{R}^2 \to \mathbb{R}$ that defines a mapping from vertices to grayscale values. Figures 2(d) and 2(e) compare local unweighted and local weighted dilation and erosion. The graph associated to these local processing is a 4-adjacency grid graph, where the weight function is w=1 for the unweighted case and $w = g_2$ with $F(f^0, .) = f^0$. As shown on these examples, weighted processing better preserves edge information and main image structures as compared to unweighted one that destroys them during morphological processes. Figure 2(f) illustrates the flexibility of our framework by employing another image graph representation that allows fast processing. Figure 2(c) shows a reconstructed image with fine partition (Fig. 2(b)) obtains from Fig. 2(a). Each pixel value in the fine partition is replaced by its surrounding region mean color value. Then, the partition is associated with a RAG where each vertex is associated with mean value function of its associated region. One can note the reduction of the simplified version as compared to the original one (82% in terms of vertices). Figure 2(f) shows dilation and erosion performed with this RAG where the weight function is the same used in the grid graph case. Results exhibit similar behaviors as compared to those in Fig. 2(e) while drastically reducing computation complexity due to the reduced number of vertices to consider.

Nonlocal processing of textured images. This experiment shows one of the novelty of our formulation: applying nonlocal patch-based approach to morphological processing. To this aim, we compare local operations and nonlocal

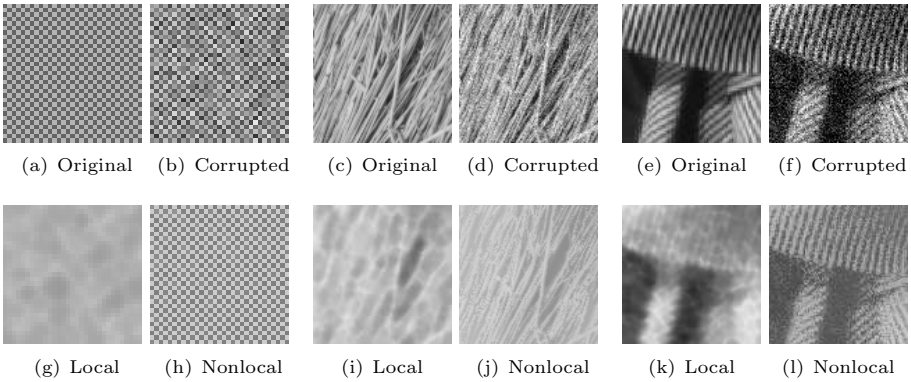

(a) Original (b) Corrupted (c) Original (d) Corrupted (e) Original (f) Corrupted

(g) Local (h) Nonlocal (i) Local (j) Nonlocal (k) Local (l) Nonlocal

Fig. 3. Local and nonlocal closing on textured images. First row: original and corrupted test images (Gaussian noise where $\sigma = 20$). Second row: local and nonlocal closing results.

configurations on textured images. Figure 3 shows the obtained results for three test images. The first row shows original images (Figures 3(a), 3(c) and 3(e)) and corrupted ones (Figures 3(b), 3(d) and 3(f)) with Gaussian noise where σ=20. The second row results are obtained by processing the corrupted images. For each test image, images at left (Figures 3(g), 3(i) and 3(k)) are results obtained with usual local closing achieved on a 4-adjacency grid graph associated with a constant weight (w=1). Images at right show results closing obtained with nonlocal configuration. These results clearly demonstrates that nonlocal patch-based configuration outperforms local approach. Nonlocal patch-based method better preserves frequent features during the morphological processing as compared to the local one that destroys fine structures and repetitive elements.

To obtain such nonlocal results, the graph structure needs to incorporate more image feature information than local one. When $f^0 \in \mathcal{H}(V)$ is the image to process, the nonlocal features are provided by image patches i.e. $F(f^0, u)$ is the values of f^0 in a square window of size $(2s+1)\times(2s+1)$ at vertex u, which we note $F_s(f^0, u) \in \mathbb{R}^{(2s+1)\times(2s+1)}$. Then, the graph constructed to obtain nonlocal patch-based closing corresponds to a modified version of k-NN (undirected) where the nearest neighbors is selected depending on a patch distance measure ρ defined as

$$\rho\left(F_s(f^0, u), F_s(f^0, v)\right) = \sum_{i=-s}^{i=s} \sum_{j=-s}^{j=s} G_a((i,j)) \|f^0(u+(i,j)) - f^0(v+(i,j))\|_2^2 \ .$$

G_a is a Gaussian kernel of standard deviation a and the final weight function associated with this graph is w=1. In experiments of Fig. 3, the graph is a 10-NN graph with $F_3(f^0, .)$ as the feature vector within a neighborhood search window of size 21×21. Similar definition and graph construction can be found in [7, 8]

and references therein.

Extension to high-dimensional unorganized data sets processing. The following experiments present a novel application of morphological operators: high-dimensional unorganized data sets processing. Figures 4 and 5 show opening operation on four synthetic independent data sets and on the United States Postal Service (USPS) handwritten digits images database.

Figure 4 shows the opening results on four noisy data sets. To obtain such results, the graphs associated to original data (Fig. 4(a)) are a modified (undirected) 8-NN graph associated with the weight function $w = g_2$, where each vertex of each graph corresponds to a data point and is described by a 2-dimensions feature vector. The four constructed graphs are shown in Fig. 4(b). Figure 4(c) shows results of opening operation. These results clearly show the filtering, denoising effect of the opening on the noisy original data. The processing tends to group the data into the feature space while preserving main data structures.

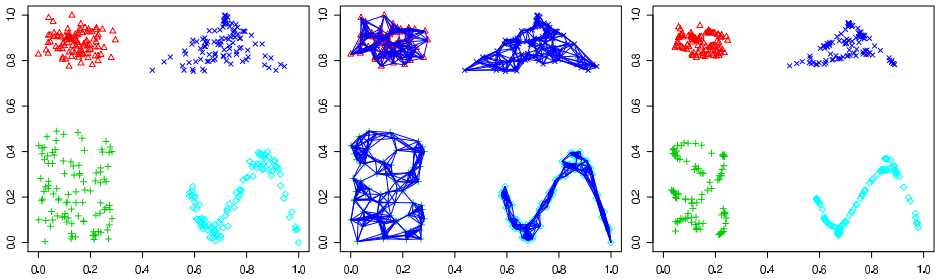

(a) Original data sets (b) 8-NN graphs (c) Opening results

Fig. 4. Opening on four independent synthetic data sets.

Figure 5 shows the processing of high dimensional real-world image manifolds: the USPS handwritten digits data set. This database consists in grayscale handwritten digit images scanned from digit 0 to 9. Each image is of size 16×16. To perform opening operation on USPS database, we use two randomly subsampled of 100 samples test sets. One from digit 0 and the other a mixed from digits 1 and 3. The graphs associated to the original data (Fig. 5(a)) are a modified (undirected) 8-NN graph associated with the weight function $w = g_1$, where each vertex of each graph corresponds to an image sample and is described by a 256-dimensions ($\mathbb{R}^{16\times16}$) feature vector where each feature is a pixel grayscale value. Figure 5(b) presents the opening results. These results clearly show the filtering effect of the opening operation where all samples tends to be uniformly identical and converge to an artificial mean digit model.

Finally, these two experiments show the potential of our morphological approach to process high-dimension unorganized data sets. This processing can be

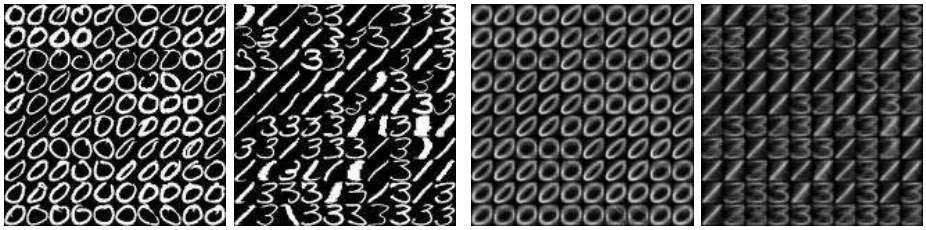

(a) Original data (b) Corresponding opening

Fig. 5. Opening on USPS digit 0 and mixed digits 3 and 1.

viewed as a data pre-processing that can be useful to improve the efficiency of final classification or machine learning purposes.

5 Conclusion

In this paper, a novel formalism of Mathematical Morphology operators based on PdEs over weighted graphs of arbitrary topology has been proposed. This provides a framework that extends PDEs-based methods to discrete local and nonlocal schemes. Moreover, this enables to process by morphological means any high-dimensional unorganized multivariate data that has been very few considered in literature. Fast morphological processing of images has also been proposed by considering the Region Adjacency Graph instead of the usual grid graph. The integration of nonlocal patch-based approach was highlighted for morphological processing as an efficient way to preserve fine and repetitive structures. Finally, our proposed framework allows us to apply morphological operations on any discrete domain that can be useful for filter and denoise manifolds or databases.

References

1. Soille, P.: Morphological Image Analysis, Principles and Applications. Second edn. Springer (2002)
2. Brockett, R., Maragos, P.: Evolution equations for continuous-scale morphology. In: IEEE International Conference on Acoustics, Speech, and Signal Processing, 1992. Volume 3. (1992) 125–128
3. Sapiro, G., Kimmel, R., Shaked, D., Kimia, B., Bruckstein, A.: Implementing continuous-scale morphology by curve evolution. Pattern Recognition **26**(9) (1993) 1363–1372
4. Maragos, P.: PDEs for morphology scale-spaces and eikonal applications. In Bovik, A., ed.: The Image and Video Processing Handbook. second edn. Elsevier Academic Press (November 2004) 587–612
5. Breuß, M., Burgeth, B., Weickert, J.: Anisotropic continuous-scale morphology. In Martí, J., ed.: In Proceedings of the 3rd IbPRIA. Volume 4478 of LNCS., Springer Berlin / Heidelberg (2007) 512–522

6. Buades, A., Coll, B., Morel, J.: Nonlocal image and movie denoising. International Journal of Computer Vision **76**(2) (february 2008) 123–139
7. Gilboa, G., Osher, S.: Nonlocal operators with applications to image processing. Report 07-23, UCLA, Los Angeles (July 2007)
8. Peyré, G.: Manifold models for signals and images. Technical report, CEREMADE, Université Paris Dauphine (2007)
9. Elmoataz, A., Lézoray, O., Bougleux, S.: Nonlocal discrete regularization an weighted graphs: a framework for image and manifolds processing. IEEE Transactions on Image Processing **17**(7) (July 2008) 1047–1060
10. Burgeth, B., Bruhn, A., Didas, S., Weickert, J., Welk, M.: Morphology for matrix data: Ordering versus pde-based approach. Image and Vision Computing **25**(4) (April 2007) 496–511
11. Postaire, J., Zhang, R., Lecocq-Botte, C.: Cluster analysis by binary morphology. IEEE Trans. Patt. Anal. Machine Intell. **15**(2) (February 1993) 170–180
12. Heijmans, H., Nacken, P., Toet, A., Vincent, L.: Graph morphology. Journal of Visual Communication and Image Representation **3**(1) (March 1992) 24–38
13. Meyer, F., Lerallut, R.: Morphological operators for flooding, leveling and filtering images using grpahs. In Escolano, F., Vento, M., eds.: In Proceedings of the 6th IAPR-TC-15 GbRPR 2007. Volume 4538 of LNCS. (2007) 158–167
14. Diestel, R.: Graph Theory. Volume 173 of Graduate Texts in Mathematics. Springer-Verlag (August 2005)
15. Chan, T., Osher, S., Shen, J.: The digital TV filter and nonlinear denoising. IEEE Transactions on Image Processing **10**(2) (February 2001) 231–241
16. Trémeau, A., Colantoni, P.: Regions adjacency graph applied to color image segmentation. IEEE Transactions on Image Processing **9**(4) (2000) 735–744
17. Von Luxburg, U.: A tutorial on spectral clustering. Statistics and Computing **17**(4) (2007) 395–416
18. Osher, S., Sethian, J.: Fronts propagating with curvature-dependent speed: Algorithms based on Hamilton-Jacobi formulations. Journal of Computational Physics **79** (1988) 12–49